Seismic modelling of coal bed methane strata, Willow Creek, Alberta

Sarah E. Richardson, Rudi Meyer, Don C. Lawton, Willem Langenberg[1]

SUMMARY

A numerical seismic modelling study of a coal zone in Upper Cretaceous sediments in central Alberta shows that seismic data with a dominant frequency of 100 Hz is required to map the coal zone and to resolve the lateral faces variations within. Shale plugs may be distinguished at these frequencies, but seismic data with a central frequency greater than 150 Hz would be necessary to resolve individual coal seams.

INTRODUCTION

The purpose of the project is to undertake a literature review and a numerical seismic modelling study to assess the feasibility of high-resolution reflection seismic surveys for coal-bed-methane (CBM) exploration and development. Effective CBM exploration requires that coal seams or zones of coal seams be mapped in detail. Although drilling can obtain detailed information at the well location, it cannot map lateral facies variations either within the coals or within the sediments that host the coals. In this project, numerical reflection seismic techniques are assessed for mapping continuity and coherence of coal zones. The model used for seismic modelling is based on coal outcrop patterns.

GEOLOGIC FRAMEWORK

The outcrop section used for the seismic modelling study is approximately 4 km long, along the north side of Willow Creek, a tributary to the Red Deer river valley, about 12 km south-east of the city of Drumheller in central Alberta, TWP28, R18W4 (Figure 1). Along this valley, the lowermost 45 to 55 m of strata of the Campanian to Maastrichtian-age Horseshoe Canyon Formation are exposed almost continuously, including a number of coal seams varying in thickness from only a few centimetres to a maximum of 1.4 m. The Horseshoe Canyon Formation represents the base of the Edmonton Group in this area, a thick clastic wedge overlying- and intertonguing-with the marine shales of the Bearpaw Formation (Irish, 1970). At Willow Creek, the uppermost Bearpaw Formation is present near the valley floor in the western part of the section, and is progressively covered near the upstream, east end of the section.

[1] Alberta Geological Survey, Energy Utilities Board

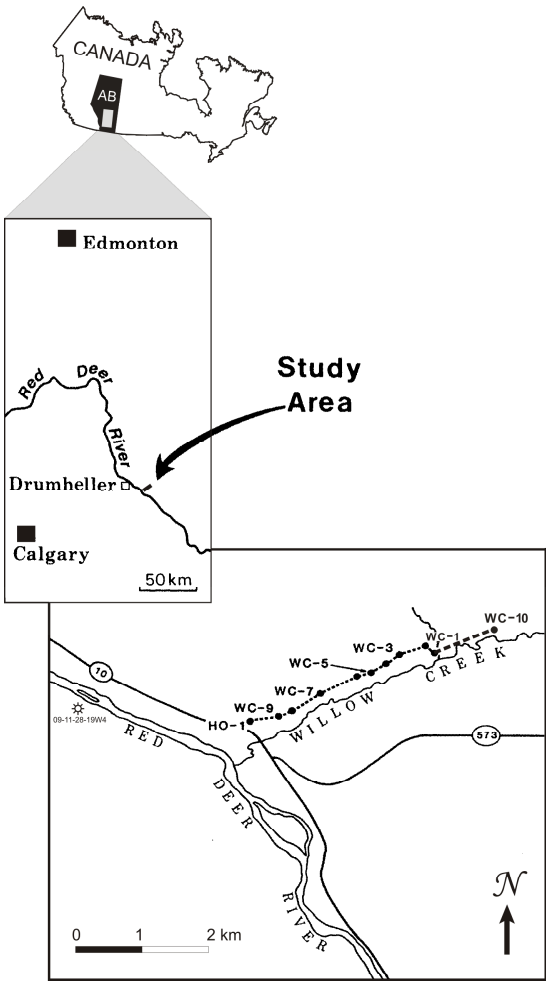

FIG.1. Location of the modelled section of about 4 km along Willow Creek. The location of HO-1 is about 14 km SE of the city of Drumheller along Highway 10 (modified after Rahmani, 1989).

Several studies have presented stratigraphic and sedimentologic details of the Willow Creek section of the lowermost Horseshoe Canyon Formation, mainly Shepeard and Hills (1970), Rahmani (1983, 1989), and Ainsworth (1994). The marine and marginal marine deposits represent a very fine-to-fine-grained, upward coarsening, SE-thickening shoreface, overlain by both sand- and mud-dominated estuarine channel deposits and associated coastal plain facies (*op cit*). Estuarine channel deposits are characterized by lateral accretion surfaces representing the inclined surfaces of migrating meander bars, and sand-mud 'doublets' and tidal bundles, likely representing tidal cycles at different temporal scales (neap-spring and semi-diurnal low and high tides, respectively, as illustrated in Figures 2 and 3. Interlaminated carbonaceous, silty shale (rooted? – Rahmani, 1989), thinly laminated/rippled fine-grained sandstone, and relatively thin coal seams characterize intertidal and supratidal coastal plain facies. Bentonitic shale intervals 0.70 to 1.80 m thick and conglomeratic shell lags ('oyster beds') are discontinuous, and preserved only locally. The interbedded sandy and muddy lithofacies and mudstone-filled channel forms add to the complexity of distinguishing intervening coal seams.

Geologists at the Alberta Geological Survey, Alberta Energy and Utilities Board provided the structural and stratigraphic framework for the modelled Willow Creek section, tied to eleven (11) stratigraphic columns using the same (or closely similar) locations and nomenclature as the cross-section presented by Rahmani (1989), in his Figure 6. Following the correlation presented, coal horizons labelled '0', '1', '4', and '5' appear to be continuous over most of the section, whereas coals '2' and '3' are clearly discontinuous. Thickness of the coal seams is rarely above 1 m. Additional discontinuous coal horizons are present between, or nearly equivalent to, coals '2' and '3' (coal '3a'), and at the east end, as multiple, very thin seams interbedded with carbonaceous shale. Locally the coals may form a sharp conformable contact with underlying sandstones (Figure 4), or may be eroded by overlying channel sandstones, occasionally preserving *Teredolites isp.* burrow traces. However, over most of the Willow Creek section the coals are associated above and below with grey-brown, carbonaceous siltstones and shales (Figures 2, 3, 4, 5).

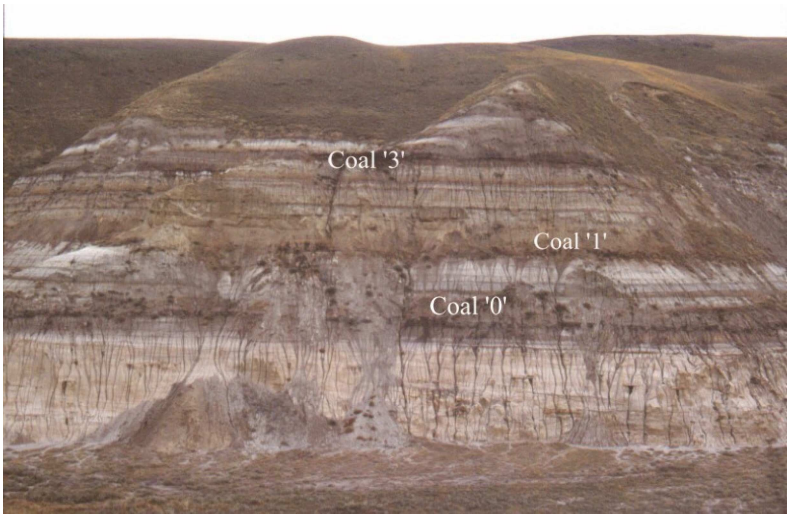

FIG. 2. Lower half of succession near West end of Willow Creek. Lower most sandy channel fill with lateral accretion surfaces overlain by coal '0' inter-bedded with carbonaceous siltstone and shale. Coal '1' in sharp contact with underlying white sandstone, and Coal '3' above brown, planar-bedded silty sandstone and shale.

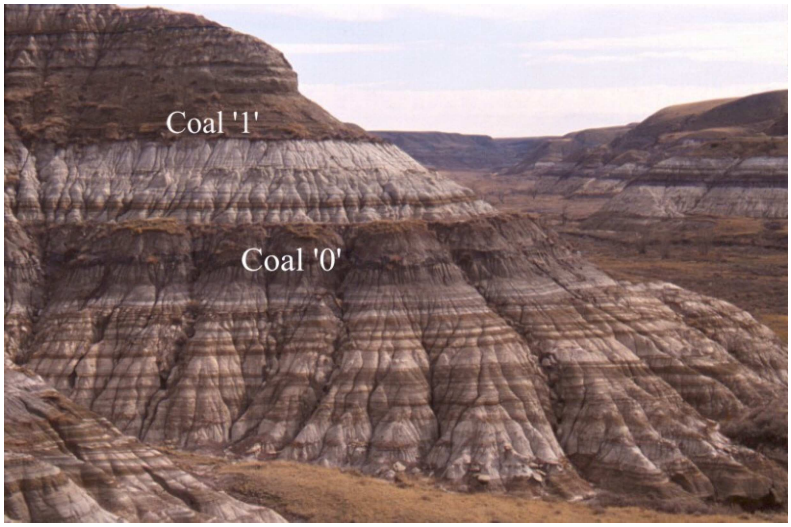

FIG.3. Muddy and sandy lateral accretion surfaces (IHS) within tidally influenced channel deposit at the base, overlain by carbonaceous, silty shale and the coal ‘0’ horizon. Coal ‘1’ is again in sharp contact with underlying white sandstone interval (North side of West-end, Willow Creek).

FIG. 4. Coal ‘1’ about 1.3 m thick. Note the thin stringers of silty shale within coal seam and sharp base with cemented top of underlying sandstone.

FIG.5. Thin coals '4' and '5' near East end of modelled section, separated by thin sandstone bed, possibly a shallow channel margin deposit or crevasse splay. Further West the two coals are separated by carbonaceous silty shale.

In addition to the cross-section, Langenberg provided a list of nearby wells and picks of sub-surface tops closely or partially equivalent to the outcrop section at Willow Creek: 14-19-28-23W4, 02-13-28-22W4, 14-28-28-20W4, 09-11-28-19W4, and 08-2727-18W4. Sonic and Density logs from segments of these wells were used to create synthetic seismograms to model the seismic response of the interval, particularly of the coals and adjacent lithologies. The closest of these wells, 09-11-28-19W4, is located about 2.5 km west of the beginning of the section at HO-1, but only includes an interval below the top of the Bearpaw Formation. Well 08-27-27-18W4 is located about 7 km SSE from the Willow Creek section and includes 20 m of the base of the Horseshoe Canyon Formation below the surface casing. The remaining wells are much further west but include equivalent sections including coals '0' and/or '2'. Well 02-13-28-22W4 has a full suite of modern well logs.

For three of the above wells, the log response of coals and adjacent lithologies is plotted on a graph of gamma ray (ºAPI) versus neutron porosity (%) to distinguish coals from carbonaceous siltstones and shales (Figure 6). Aside from the coals themselves, the data points plotted include 1m above and 1m below the corresponding coal seams. Very few of the coals have the very low GR (< 30–40 ºAPI) *and* high $Ø_{neutron}$ (> 60 %) characteristic of relatively clean, pure coals (shaded area in Figure 3), Rider (1996). Instead, the coal seams contain varying proportions of clays and silt, likely introduced by episodic flooding of paleo-swamps during high tides in adjacent salt-water marshes (the latter represented by the carbonaceous, silty shales above/below coals). Clearly, the shaly/silty character of the coals is an important factor in the subsequent modelling, as it will tend to obscure seismic distinction of the upper and lower contacts of coals from adjacent shales.

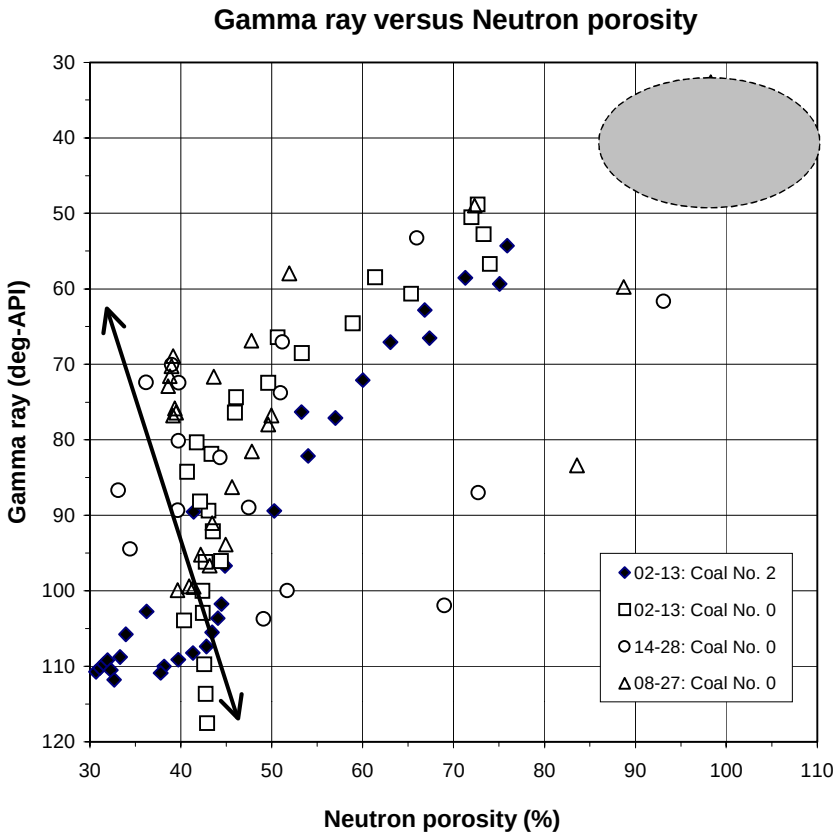

FIG. 6. Plot of gamma ray versus neutron porosity for four coal seams from three wells, stratigraphically equivalent to coals '0' and coal '2' as defined in the Willow Creek section. The area shaded in grey highlights relatively clean, pure coals. The double-headed arrow defines an approximate sand/silt to shale line, from low GR/low neutron porosity to high GR/high neutron porosity. The large number of points between the arrow and the shaded grey area correspond to coals with varying proportions of silt and clays.

LITERATURE REVIEW

In the last thirty years, considerable research has been published regarding coal-bed exploration seismology. The use of seismic surveys in coalfields has led to great improvements in effective mine planning. These techniques may also be applied to the exploration for coal bed methane.

It is essential to first distinguish between seismic resolution and seismic detection. The limit of resolution is the minimum thickness of a bed in which the top and basal surfaces produce effects that may be distinguished separately [Greaves, 1984]. The limit of resolution is dependent on the linear frequency bandwidth (not that measured in octaves), and is traditionally defined as $\lambda/4$, where λ is the wavelength corresponding to the dominant frequency of the propagating seismic wavelet. The limit of detection is the minimum thickness of a bed such that its seismic response may be distinguished at all [Greaves, 1984]. This value is dependent on signal-to-noise ratio, and is often approximately $\lambda/30$. Coal is a very unusual rock type, as it

has low seismic velocity and low density with respect to its bounding strata. As such, it often exhibits different seismic behaviours than other sediments. Gochioco (1991b) notes that, although coal seams are extremely thin with respect to seismic wavelength, their exceptionally large acoustic impedance contract with surrounding rocks results in distinct reflections. Often the limit of resolution of coal beds is closer to $\lambda/8$ rather than $\lambda/4$. Because of this large acoustic impedance contrast, the limit of detection of coal seams is also less than that for other strata, and may be as small as $\lambda/40$ (Gochioco, 1992).

Prior to Gochioco's observations, Widess (1973) questioned, "How Thin is a Thin Bed?" He concluded that in beds where the two bounding media have the same acoustic impedance, the amplitude of the reflection is approximately proportional to the bed thickness, and inversely proportional to λ. Thus, changes in reflection amplitude may be used to determine the thickness of a bed that is smaller than $\lambda/8$.

Models and simulations of coals conducted in the time domain demonstrate thinnest resolvable layers of 0.75-1.0 m. This restriction of minimum thickness may be removed by working in the frequency domain (Hughes & Kennett, 1983). A study of the seismic response of thin-bed sequences conducted in the frequency domain shows that in cyclic thin-bed structures, the composite transmission effect of peg-leg multiples becomes larger than the direct arrivals. This leads to a complex interference pattern, and difficulty in interpreting a coal response as a single geologic horizon (Hughes & Kennett, 1983). A case study of cyclothems determines that "where seams and interfaces are numerous, interference reflections are dominated by short-lag or intrabed multiples, so latter primaries have little significant influence" (Gochioco, 1992). Sophisticated interpretation techniques are needed to dissect these composite reflections. Computer modelling may be of great assistance in properly identifying these interference reflections and avoiding misinterpretation. A study by Knapp (1990) of the vertical resolution of cyclothems determined that frequencies greater than 500 Hz are needed to resolve individual cyclothem beds. Lower-frequency data may be phase-filtered, however, such that each bed has a single wavelet associated with it, that is, peaks and troughs for alternating layers.

Seismic surveys of coalfields are not only useful for interpreting bed thickness, or the overall field geometry and structure. Seismic data may allow for the identification of facies changes, which in turn may be used to determine the depositional environments of coals (Lawton, 1985). Knowledge of the depositional setting is useful in predicting a coal's type, quality (rank), and lateral continuity.

Fracturing and stress are essential to coal-bed methane production, as there is no matrix permeability in coal seams. Shear wave seismic data may be used as a method of fracture detection in coals (Thomsen et al., 1995). This technique originally used to detect fractured "sweet spots" in carbonates and clastics proves to be very useful in determining anisotropy in coal bed sequences. Thomsen et al. determine that R_a, a dimensionless measure of coal bed sequence anisotropy, is quite sensitive to anisotropy within the coal (i.e. fracturing), and nearly independent of the sequence geometry (i.e. the positions of the coal beds).

Before conducting a seismic survey of any area, it is essential to have an understanding of the capabilities and limitations of the equipment involved. Knapp and Steeples (1986) provide a practical overview of the many different elements involved in a seismic survey, the options available, and the applicability of various equipment and techniques to different exploration settings. A wide variety of case studies have also been published, each of which gives the details of its survey geometry.

A case study of the Highvale-Whitewood coalfield in the plains of Alberta demonstrates two important results. Firstly, the seismic survey was useful in examining field structure, determining coal thickness, and identifying surrounding strata (Lyatsky & Lawton, 1988). The study demonstrates that the character of coal reflections is not always related to geological variations within the coal, but is also dependent on the influence of the overlying and underlying sediments (till and sandstone in this instance). Secondly, synthetic seismograms of the area based on density logs alone are very similar to those based on combined sonic/density data (Lawton & Lyatsky, 1991). These density-only synthetics are very similar to the real seismic data collected in the field, as well, suggesting that density logs alone may be used to seismically model coal beds. This is particularly useful in Alberta, where well density logs are far more common than sonic logs.

Very high frequency and high bandwidth data is desirable to adequately image thin coal seams, and has been successfully collected in some relatively shallow surveys. A case study of such a survey in Wyoming demonstrates the effectiveness of high frequencies in imaging the Wyodak coal seam, as well as a previously undetected sandstone-filled incision (Greaves, 1984).

The Sydney basin (Australia) is the location of another shallow seismic reflection survey. This case study proposes that the key to improved resolution is maximizing signal bandwidth and dominant frequency, while minimizing all related noise (Greenhalgh et al., 1986). Explosive sources detonated beneath the weathered layer (such as those used in Vertical Seismic Profile collection) are the best source of high frequencies. The VSPs in the study area illustrate the interference effects of multiple coal seams. The usefulness of Vertical Seismic Profiles is also examined in the US Appalachian coal basin (Gochioco, 1998). Correlation of a VSP to the related seismic section helps to assure that the reflection associated with the target seam is correctly interpreted. VSP data may be particularly useful in areas where checkshot data or geophysical logs are unavailable.

Fault identification has been another advantage of seismic data in areas of coal production. Faults are of great importance in mine design, and may also interfere with coal bed methane production if the throw is greater than the seam thickness. A survey of the Carbondale formation (within an unidentified U.S. mine) allows the identification of faults with displacement of the same magnitude as the seam thickness (Gochioco & Cotton, 1989). Surveys conducted near Harco, Illinois, allowed the identification of eight previously undetected faults, as well as the proper location of a sandstone-filled incision (Henson, Jr & Sexton, 1991). This study demonstrated the effectiveness of combined seismic and borehole data, as the incision

had been incorrectly mapped using borehole data alone. A second study within the Illinois basin (Gochioco, 2000) demonstrates the increased effectiveness in using 3D seismic data over 2-D. Misinterpretations may occur when geologic anomalies are small relative to the spatial resolution of a 2-D survey.

The Cedar Hill field, in the San Juan basin, is currently producing coal-bed methane. Its development relied on the assumption of a homogeneous field. Multi-component 3D seismic data has since shown the field to actually be compartmentalized, and heterogeneous (Shuck et al, 1996). Compressional-wave data is useful for mapping structure and identification of overpressured zones. When P-wave data is combined with petrophysical and reservoir engineering studies, it is possible to identify isolated pressure cells, zones of increased fracture density, variable fracture directions, and the strike-slip faults that compartmentalize the reservoir. Proper identification of features such as these allow for more suitable development planning.

This same multi-component 3D survey in the Cedar Hill field has been examined in conjunction with amplitude-vs.-offset (AVO) analysis (Ramos & Davis, 1997). Areas with large AVO intercepts indicate low-velocity coals, possibly related to zones of stress relief. Large AVO gradients are indicative of large Poisson's-ratio contrasts, and therefore, are indicative of high fracture densities. The integration of multi-component 3-D seismic and AVO analysis yields a useful approach to characterizing fractured reservoirs.

Not all studies involving coal exploration seismology are success stories, however. A study of the Belvoir coalfield in England applied generalized linear inversion to reflection data to test whether accurate values for coal-seam thicknesses could be obtained (Gang & Goulty, 1997). Inversion produced fairly good results when testing for the continuity of coal seams, but showed variations in coal seam thicknesses that are geologically implausible. In order to accurately apply this inversion technique, better suppression of residual multiple activity, improved signal-to-noise ratio, and a broader data bandwidth are needed.

The wide variety of case studies effectively demonstrates the many advantages of coal exploration seismology. Whether examining mine development or coal-bed methane production, a seismic survey is an invaluable tool.

SYNTHETIC SEISMOGRAM MODELLING (1-D)

LogM Well Editor software was used to create 1-D synthetic seismograms of two different well-log suites. These wells are located near the Willow Creek study area, and were selected because they had digital sonic logs. Although there are a number of wells close to the study area, sonic logs are essential as a time-control curve. A frequency series of synthetic seismograms was created, using a Ricker wavelets ranging from 30 to 310 Hz dominant frequencies. Convolution was performed using both a minimum-phase and zero-phase wavelet.

Above the limit of resolution, the coal seams should be represented seismically by a trough at the upper contact of the coal and by a peak at the basal contact. The frequency at which each coal seam becomes resolvable is dependent not only on its thickness but also on the level of contrast with the overlying/underlying rocks. (For instance, a shaly coal overlying shale is not as easily distinguishable as a coal overlying silts). The thickness of the surrounding beds also seems to be a factor: that is, a thin bed surrounded by thick homogeneous beds will be distinguished at a much lower frequency than one that is surrounded by thin beds of varied lithology. This is the result of interference generated by intrabed multiples in thin-bedded sequences.

Well 9-11-28-19W4

In the illustrated sample results of the 1-D modelling of this well (Figures 7, 8), the three synthetic seismograms are always based on (1) Sonic alone, (2) Sonic + Density, (3) Density alone. Coal tops only are indicated on the well logs, no coal bases.

Two coals, named “Coal X” and “Coal Y”, have been identified. Coal X is at 182.37 m depth, and is 2.23 m thick. Coal Y is at 207.83 m depth, and is 1.56 m thick. Both are underlain and overlain by silts, though Coal Y exhibits greater velocity/density contrast with its overlying sediments than Coal X shows. Table 1 indicates the frequency at which each coal may be distinguished on the synthetic seismogram.

Synthetic parameters	Coal X	Coal Y
Minimum Phase/Sonic	250 Hz	210 Hz
Minimum Phase/Sonic + Density	210 Hz	190 Hz
Minimum Phase/Density	190 Hz	170 Hz
Zero Phase/Sonic	230 Hz	230 Hz
Zero Phase/Sonic + Density	230 Hz	250 Hz
Zero Phase/Density	190 Hz	210 Hz

Table 1. Frequency of wavelet at which coals may be distinguished seismically

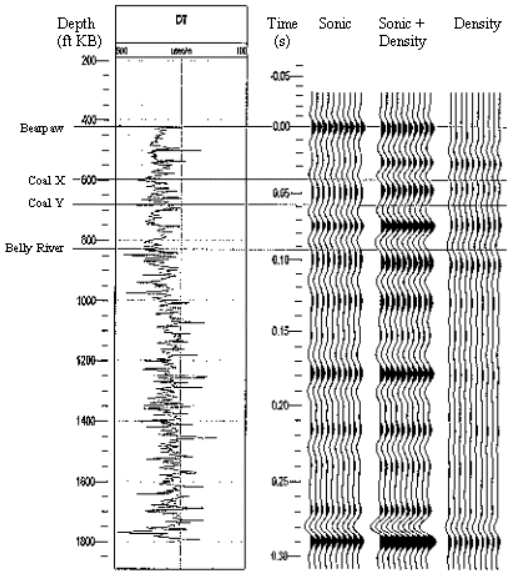

FIG. 7. Synthetic seismograms for well 9-11-28-19W4, created using a 30 Hz zero-phase Ricker wavelet.

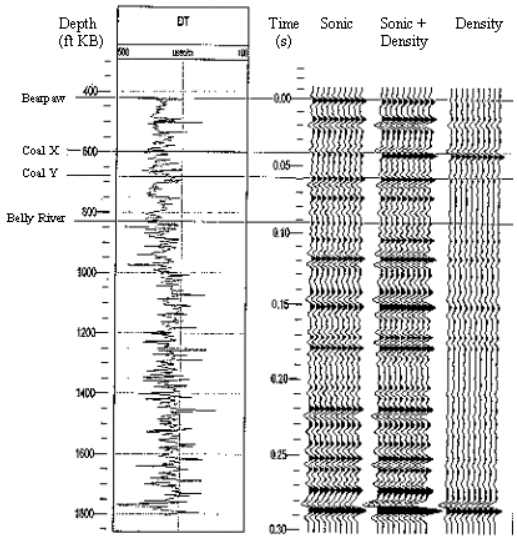

FIG. 8. Synthetic seismograms for well 9-11-28-19W4, created using a 90 Hz zero-phase Ricker wavelet.

Well 2-13 28-22W4

No density log is available for this well; all synthetic seismograms (Figures 9, 10) are based on the sonic log alone. Coal labels on the log indicate the tops of coals; no bases are indicated.

This well contains eight separate coal seams, named according to the given well picks. These coals vary in thickness from 1.01 m to 3.36 m. This thickest coal is actually a combination of three coal seams (numbers 3, 4, and 5) that are separated by shaly coals. Coal 2 and Coal 0 correspond to coal seams present in the Willow Creek outcrop section. All other coals, designated "SS", are subsurface relative to the outcrop.

Coal name	Thickness	Minimum Phase	Zero Phase
Coal 2	1.25 m	210 Hz	170 Hz
Coal 0	2.12 m	170 Hz	150 Hz
SS Coal 2	1.29 m	190 Hz	190 Hz
SS Coal 345	3.36 m	190 Hz	150 Hz
SS Coal "shaly"	1.03 m	---	Top 250 Hz
SS Coal 10	1.71 m	190 Hz	110 Hz
SS Coal 18	1.01 m	210 Hz	130 Hz
SS Coal 21	1.05 m	230 Hz	190 Hz

Table 2. Frequency of wavelet at which coals may be distinguished seismically

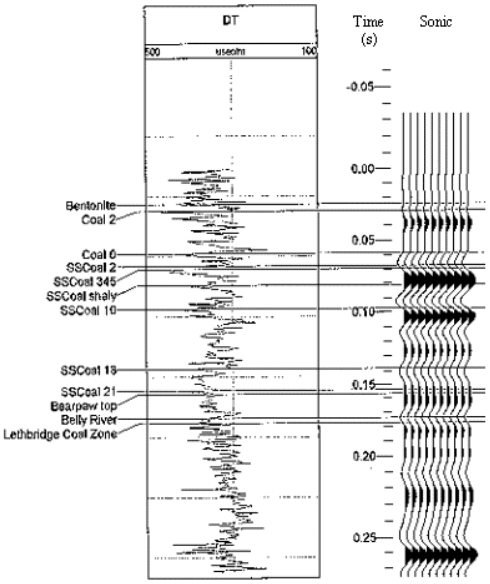

FIG. 9. Synthetic seismograms for well 2-13-38-22W4, created using a 30 Hz zero-phase Ricker wavelet.

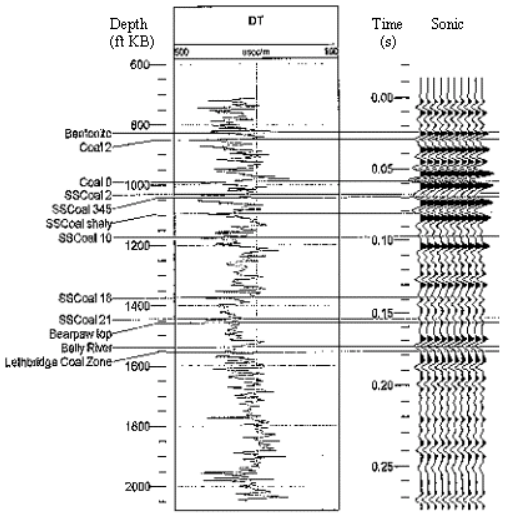

FIG.10. Synthetic seismograms for well 2-13-38-22W4, created using a 90 Hz zero-phase Ricker wavelet.

Observations

Minimum Phase vs. Zero Phase

On the whole, there are few differences between the zero-phase (no samples shown here) and minimum-phase synthetic seismograms. The differences between the two include:

- Amplitude of peaks and troughs is generally greater in minimum-phase models
- Slight differences in peak/trough configurations e.g.
- Events occur later (1-2 ms) in minimum-phase model (well 9-11, 30 Hz)
- Apparent phase reversal (same event is peak in one, trough in other)
- Peaks/troughs change shape, such as peaks becoming double peaks
- As frequency of wavelet increases, configuration differences decrease
- Generally, minimum-phase shows a greater number of events (i.e. more peaks/troughs) than zero-phase.

Sonic alone vs. Sonic + Density vs. Density alone

- Sonic + Density shows greatest amplitudes
- Density alone shows same events, but amplitude greatly reduced
- Time of some events differs slightly (1-2 ms)
- As frequency of wavelet increases, the density-alone model shows fewer and fewer events (whereas others show more and more), only the strongest events continue to be visible
- At highest frequency wavelets, the only strong peaks in the density only model result from the coal seams.

Thus, the sonic + density seismograms produce the best model overall, but when imaging coal seams, seismograms based on density logs alone may be adequately effective. These density-only synthetic sections highlight the coals, but give little information about the surrounding lithologies.

SYNTHETIC SEISMIC SECTIONS (2-D)

The digital model used in GXII modelling is based on a hand-drawn cross-section of the Willow Creek study area. This cross-section was digitized and appropriate layer parameters have been added. P-wave velocity values are based on sonic logs of related sediments. Seismic modelling was conducted on three variations of this model. The first is the original section, with approximately 40 m of overburden above the uppermost coal seam. The second added 200 m of overburden, and the third used 400 m of overburden. Raising the uppermost layer of Quaternary sediments and inserting a layer of "average" silt produced the second and third models. This thick layer is modelled as a homogeneous unit containing no reflectors. The original 40 m Willow Creek model is illustrated in Figure 11.

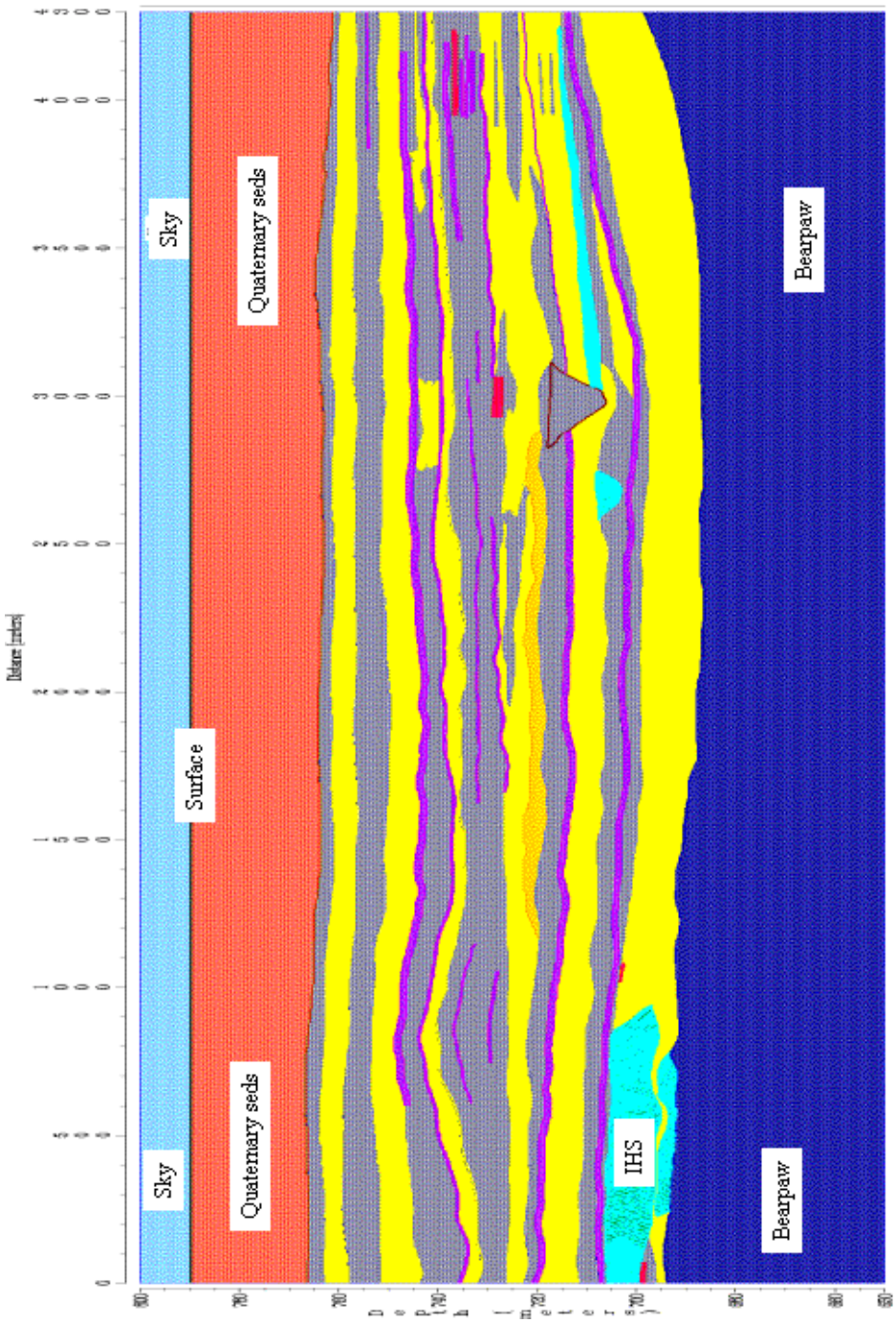

FIG. 11. ‘40 m’ model used for 2D seismic simulations. Layer parameters are in Table 3.

Layer Name	Colour	P-wave velocity
Sky	Light Blue	N/A
Quaternary	Orange-Red	2000 m/s
Shale	Grey	2750 m/s + 0.1 m/s/m
Sandstone	Yellow	2850 m/s + 0.1 m/s/m
Coal	Purple	2500 m/s
Bentonite	Red	2450 m/s
Oyster Beds	Orange-Yellow	2775 m/s
IHS sand	Cyan	2800 m/s
IHS shale	Green	2770 m/s
Bearpaw	Dark Blue	2700 m/s
"Average" silt	N/A	2800 m/s

Table 3. Parameters used in Willow Creek Model

Ray tracing was conducted using both Normal Incidence (NI) and Common Midpoint (CMP) algorithms. Rays were converted to traces by convolving with Ricker wavelets of varying frequencies. The 40 m model uses wavelets of 50, 100, and 150 Hz. The two deeper models are also modelled using these three wavelets, though the 50 and 100 Hz convolutions will be more reliable than the 150 Hz section, as higher frequencies are severely attenuated at such depths.

The large number (>1600) of IHS beds results in extremely large computing times. Time constraints prevented the inclusion of IHS in the CMP ray-tracing algorithms. For simplicity, a single layer with a P-wave velocity of 2785 m/s replaces IHS units. It is assumed that the IHS would have a similar seismic response when modelled using CMP ray tracing as that resulting from NI ray tracing.

The strongest reflection in each simulation results from the interface of Quaternary sediments with underlying strata. To keep this event from overshadowing the desired study area (the coals and IHS), it has been removed from the ray tracing simulations. When left in, it generates a strong peak at approximately t=20 ms.

Coal seams in the study area have a low apparent reflectivity because they are so thin. The reflectivity of the thin coals is approximately equal to that of the sandstone/shale interfaces in this model. Often a coal seam acts as the divider

between sandstone and shale units, or within 2 m of a sandstone/shale contact. As such, the reflectivity of the coals is often added to that of a contact, resulting in a single combined response.

IHS is very difficult to image seismically. The combination of so many thin beds results in an acoustically transparent unit. IHS units are detectable, but individual beds within each unit are much smaller than the limit of resolution.

Normal Incidence Modelling

Zero-offset, or normal incidence, modelling was conducted twice on all three models. The first set of ray tracing calculated reflections only, whereas the second set included reflections and diffractions. All normal incidence simulations were conducted using source/receiver spacing of 2.5 m from x=0 to 4300 m.

The unprocessed results are examined as well as migrated data. Sections included for illustration include reflections and diffractions. Kirchhoff migration was used, applying constant velocity of 2800 m/s, a value approximately equal to the average velocity of the entire section. Velocities of 2750 m/s and 2850 m/s were also tested, but showed no discernable difference.

40 m Model

A synthetic sonic log was created using a velocity profile from x = 850 m (at approximately the crest of the anticline at the West end of coal 4). The thicknesses and velocities of sediments used in the GXII model generated this "synthetic log" which was convolved with a wavelet in LogM to assist in the identification of seismic events resulting from the ray tracing.

Modelling the 40 m model with a 100 Hz wavelet (Figure 12) results in an immediately obvious improvement in resolution over the 50 Hz model. Coal 1's response is strong and continuous, and the shape of the incising mud plug is clearly visible. Coal 2 still appears as a continuous reflector, although there is a suggestion of its discontinuity between SP 950 and SP 1050.

Underlying the coal 4 anticline is the first detectable, though weak, response of coal 3. The responses of coals 4 and 5 still combine to produce a single seismic event. A pair of strong continuous reflectors overlies this combined response, and is the result of sandstone/shale interfaces.

Noise is present throughout the IHS units, but is confined, and does not interfere with surrounding events as much as in the 50 Hz model.

The processed 100 Hz section (Figure 12) is very similar to the raw data except within the IHS units. Migration of this data eliminates IHS-generated noise entirely, demonstrating the importance of examining both raw and processed data. The absence of noise has rendered detection of IHS impossible on the migrated

section. Migration also results in a weaker, less continuous reflection from the upper Bearpaw contact.

Coals 4 and 5 are detectable separately when the section is convolved with a 150 Hz wavelet (Figure 13, post-migration). Coal 5 terminates abruptly at ~SP 225, and the sandstone/shale interface that accompanies it is detectable to the West. The change in character (e.g. lesser amplitude) of this Western event indicates a lithological contrast to coal 5. Discontinuous coal 3 is evident throughout the section, not just underneath the coal 4 anticline. The discontinuous nature of coal 2 becomes more readily visible, and its response is separate from the sandstone/shale response in some areas, most notably between SP 800 and 1050.

The upper surface of the IHS unit East of the mud plug is resolvable, and is the first indicator of IHS other than noise. Unfortunately, without the noise (post-migration), this event is indistinct from other sedimentary contacts. The presence of the unit may be detected, but its nature may not.

Elimination of IHS noise and collapsing of the few diffraction hyperbolae are the key distinctions between migrated and raw 150 Hz data.

For the sake of interest, the 40 m model has also been convolved with 250 Hz and 500 Hz wavelets. These frequencies are not attainable in field experiments, but provide a fascinating contrast to the lower frequency sections. Nearly all lithology interfaces are resolvable, and distinct events for the upper and lower contacts of coals may be interpreted. At a dominant frequency of 500 Hz, the difference in character between coal responses and sand/shale responses becomes more apparent. Coal-related events in general have larger amplitudes and are “stronger”-looking than those related to other strata.

200 m Model

The 200 m model traces created with a 100 Hz wavelet (Figure 14) are very similar to those of the 40 m model. The most obvious difference between the two is the sharp increase in diffraction hyperbolae present within the deeper section. IHS noise is worse in the 200 m model, and there are changes in the character of events. The uppermost sandstone/shale interface response has less amplitude in the deeper model, although the coal responses remain similarly strong. Overall, the same events are detectable or resolvable on each section.

Migration of this model removes the hyperbolae and IHS-generated noise. Events are actually more difficult to identify post-processing, as the inverted diffraction hyperbolae interrupt a number of horizons. No indication of the mud plug is visible, and there is considerable wavelet noise in the upper portions (100-140 ms) of this section.

When convolved with a dominant frequency of 100 Hz, coal seams become more detectable, and a number of interfaces are easily interpreted than in the 50 Hz convolution. The first indication of coal 3, beneath the coal 4 antiform, appears, and

the shape of the mud plug is weakly visible. The discontinuous nature of coal 2 is suggested by its response at this higher frequency. IHS noise remains prevalent, and diffraction hyperbolae interfere with interpretation.

Interpretability is improved with migration (Figure 14). The shape of the mud plug is clear, IHS noise is eliminated, and many events are more continuous as a result of collapsing hyperbolae. The response of the upper surface of the IHS unit West of the mud plug is discernable, although no character suggests its unique composition.

Dominant frequencies of 150 Hz are likely unattainable at depths of 200 m, however, this migrated model (Figure 15) is included for reference. Improved resolution allows coals 4 and 5 to be identified separately, as well as all discontinuous portions of coals 3 and 2. Coal 5 may once again be seen terminating abruptly (SP 225), with its associated sandstone/shale contact continuing to the West. Migration once again reduces diffraction interference, eliminates IHS noise, and produces a slightly clearer section.

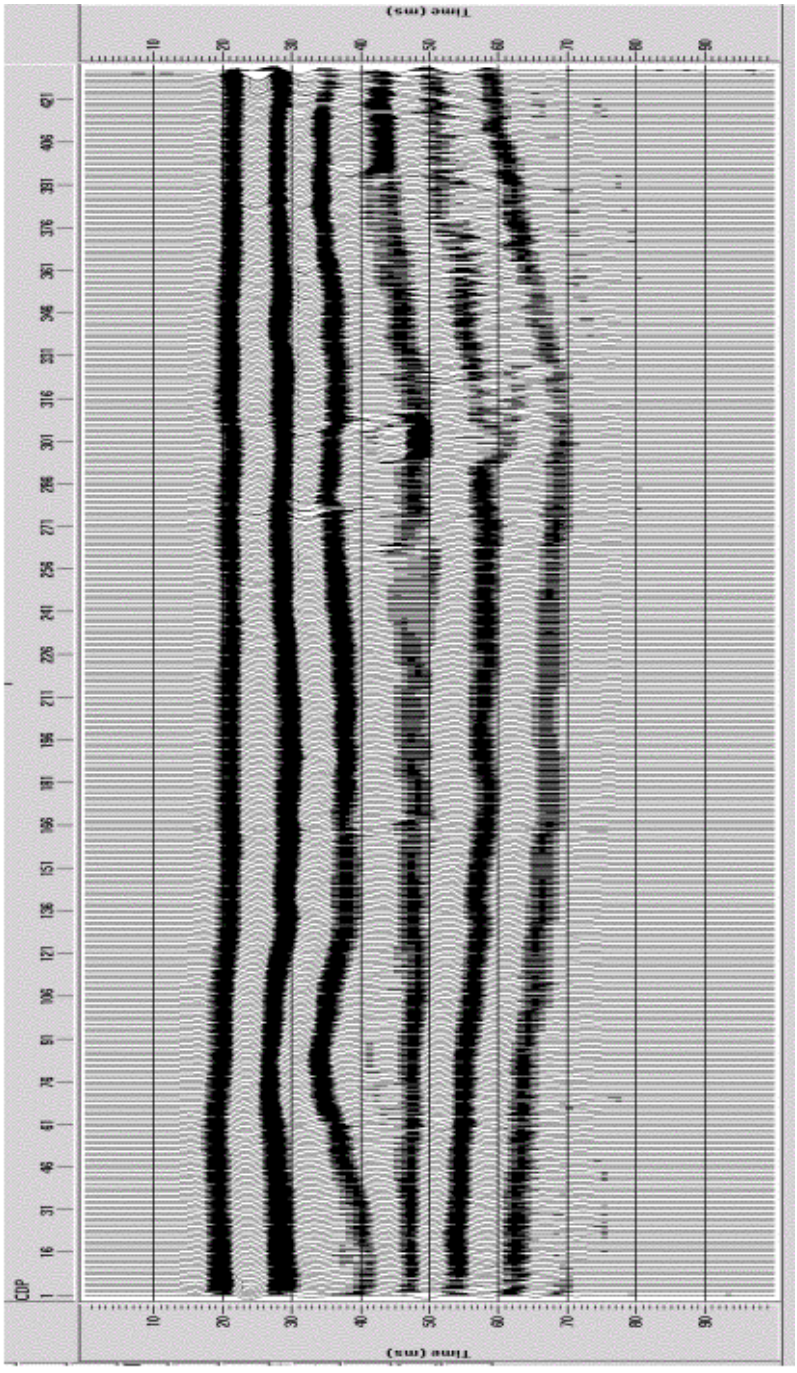

FIG. 12. Seismic traces created with 40 m model, normal incidence ray tracing, 100 Hz wavelet, and migration.

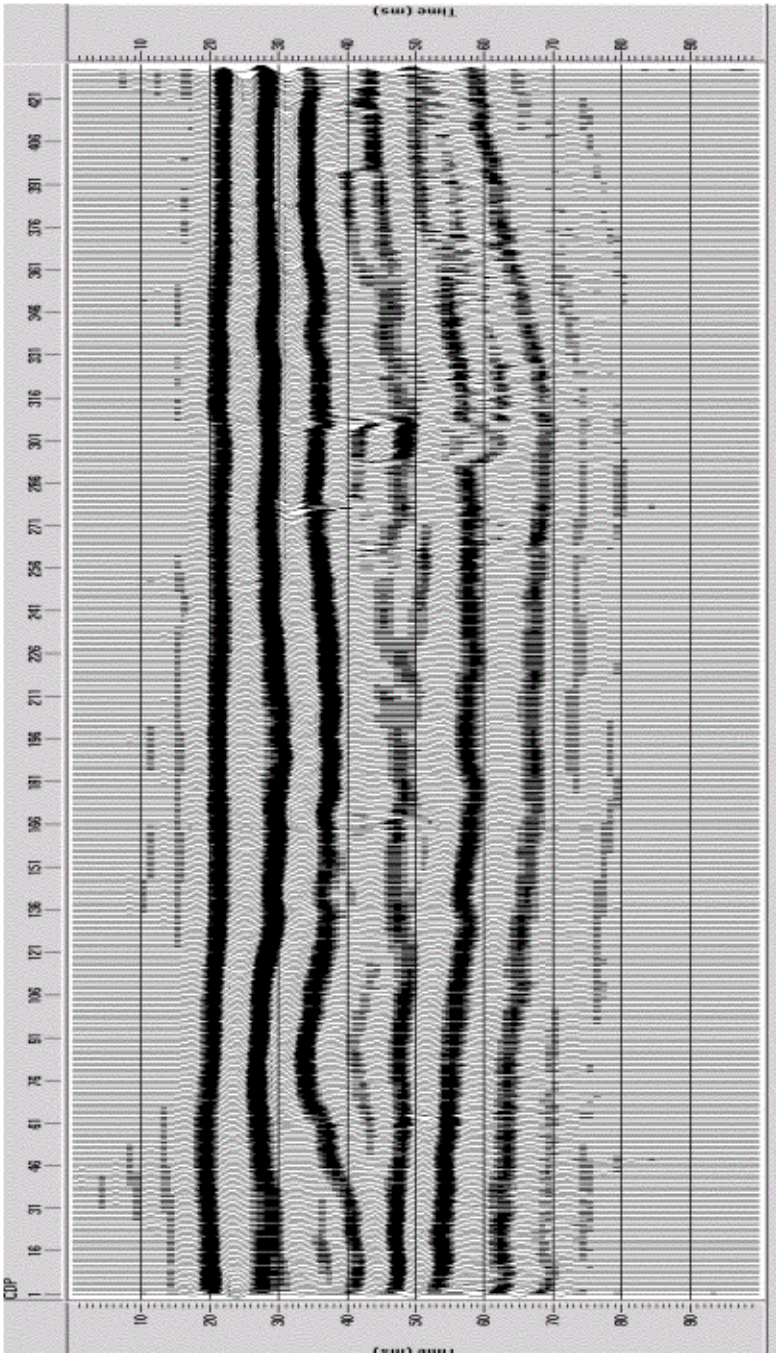

FIG. 13. Seismic traces created with 40 m model, normal incidence ray tracing, 150 Hz wavelet, and migration.

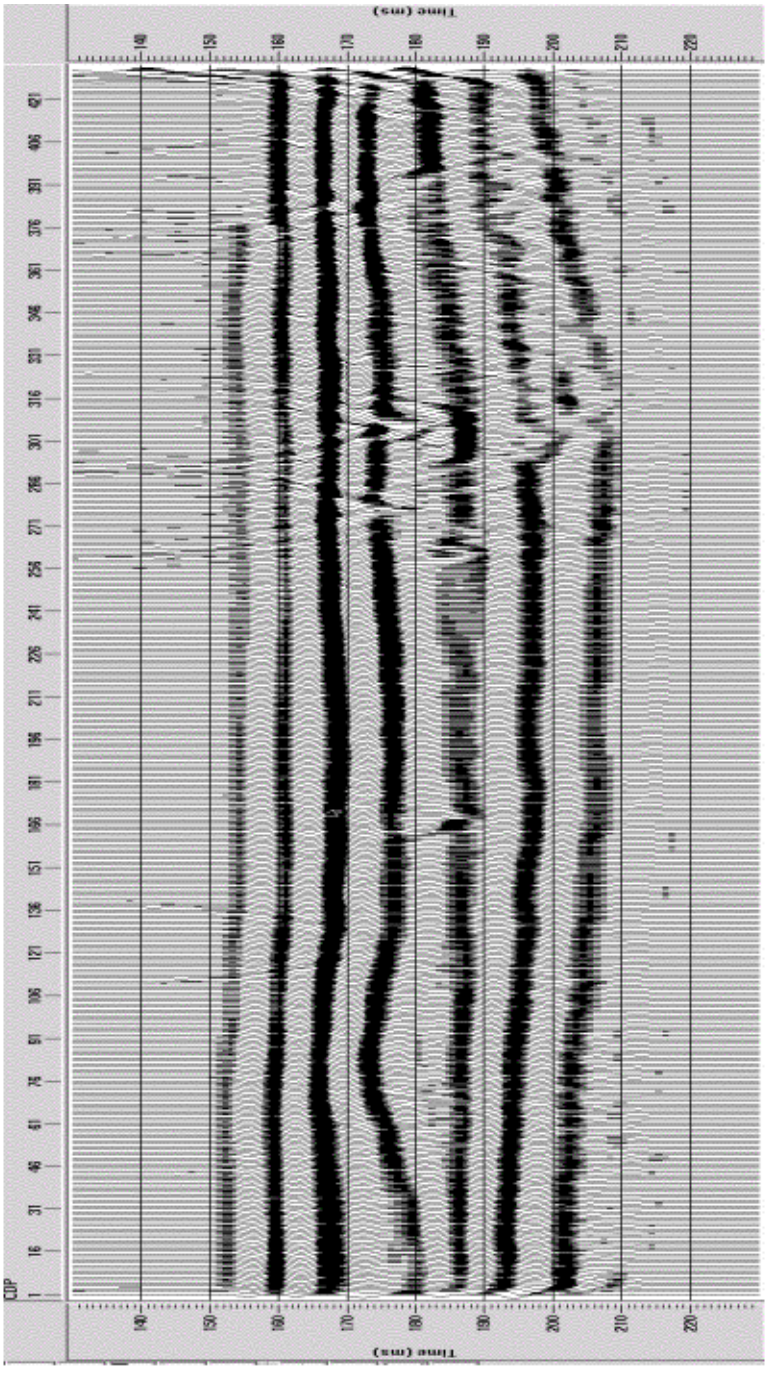

FIG. 14. Seismic traces created with 200 m model, normal incidence ray tracing, 100 Hz wavelet, and migration.

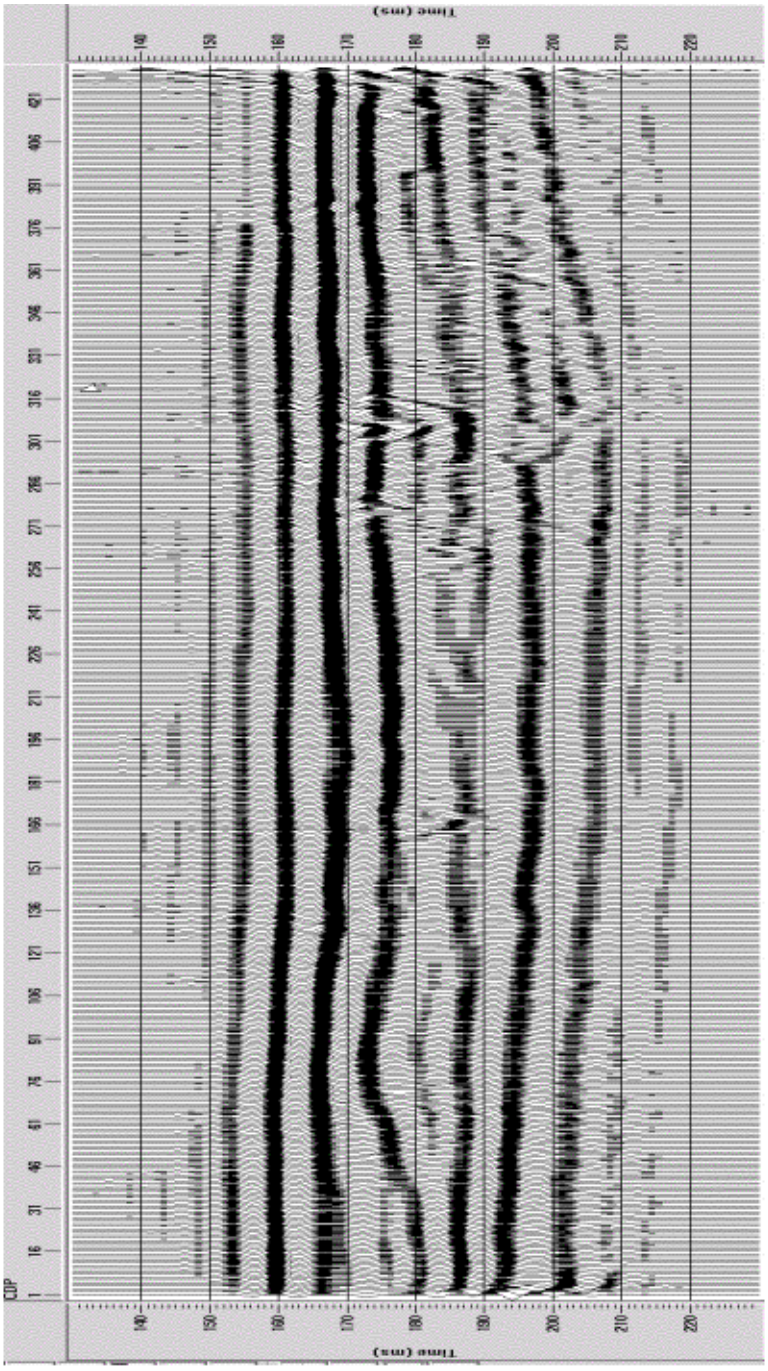

FIG. 15. Seismic traces created with 200 m model, normal incidence ray tracing, 150 Hz wavelet, and migration.

400 m Model

Events on the raw 400 m data are nearly identical to those in the shallower models. Key differences include an increase in diffraction hyperbolae, and the accompanying decrease in interpretability. Non-coal responses, such as that of the uppermost sandstone/shale interface, are more attenuated than their equivalents in shallower models. Migration produces a section containing considerable wavelet noise. Events are difficult to interpret or identify, and continuity is compromised by the inverted hyperbolae. Only the strongest events, such as the response of coal 0, easily correlate to their equivalents in the 40 m or 200 m model. On the whole, the 400 m sections display nearly all the same events as the 200 m or 40 m sections, but are more difficult to interpret.

Common Midpoint Modelling

The common midpoint (CMP) method of ray tracing was only conducted once on each model, simulating reflections only. This is largely a result of time constraints, as common midpoint modelling is a much slower process than normal incidence modelling. The 40 m Willow Creek section was modelled using a 10 m CMP separation, and 10 offsets per side with an offset increment of 5 m. The 200 m model used 10 m CMP separation, with 15 offsets per side at 10 m increments. A 10 m CMP separation was also used in the 400 m model, but had 25 offsets per side at 10 m offset increments. As zero-offset surveys are not possible in the real world, common-midpoint ray tracing provides a more accurate simulation of a potential field survey. Common midpoint modelling includes AVO effects, for instance, which do not occur in zero-offset tracing.

Detectable events on the CMP models are essentially the same as those visible in the equivalent NI sections. The nature of these events is slightly changed, however. In the 40 m 50 Hz model, the uppermost sandstone/shale interface response exhibits lesser amplitude. Several other events are also marked by a reduced amplitude, such as the combined coal 4/coal 5 response, and the coal 2 response. The event representative of coal 1 is a weak reflection in the NI model, and is weaker still when modelled by CMP ray tracing. Slightly more interference is present within CMP sections, in this case most notably surrounding the location of the mud plug. The response of coal 0 is nearly identical to that obtained by NI ray tracing, with the exception of increased interference at SP 100. This particular interference pattern is likely the result of the edge of an IHS unit.

The lack of diffractions reduces the differences between raw data and migrated data in the CMP sections. A comparison of the 40 m 100 and 150 Hz migrated sections (Figures 16,17), however, shows differences that stem from other sources than the lack of diffractions. The shape of the mud plug is not at all definable, whereas NI ray tracing delineated it at a lower frequency of 100 Hz. Coal 1's response is quite varied between NI and CMP migrated sections. The NI model shows a clear splitting of the event to delineate both the coal and the upper surface of the IHS unit, whereas the CMP ray tracing results in a double peak that splits only slightly at the Westernmost edge of the section. The amplitude of this same event

East of the IHS unit is stronger on the CMP section, unlike the majority of reflectors, which exhibit reduced amplitude. Coal 0's response is also increased, whereas coal 3's response is reduced so severely that it is nearly undetectable under CMP modelling.

Overall, the key differences between NI and CMP modelling are slight amplitude variations and increased interference in CMP sections. Although diffractions are not included in this set of CMP modelling it can be assumed that the quantity of diffractions increases with depth just as it does in NI modelling.

Common midpoint ray tracing produces more accurate models of real-life seismic data, although it is easier to identify events on zero offset sections. For this reason, it is best to use both methods in combination. This modelling exercise has demonstrated that coals, when very thin, may be seismically detectable, but are rarely resolvable. Thin-bed coal responses are often combined with the response of surrounding interfaces. Identification of such a combined response may be facilitated by the construction of a fake sonic log in the area of interest, which may be used to create synthetic seismograms.

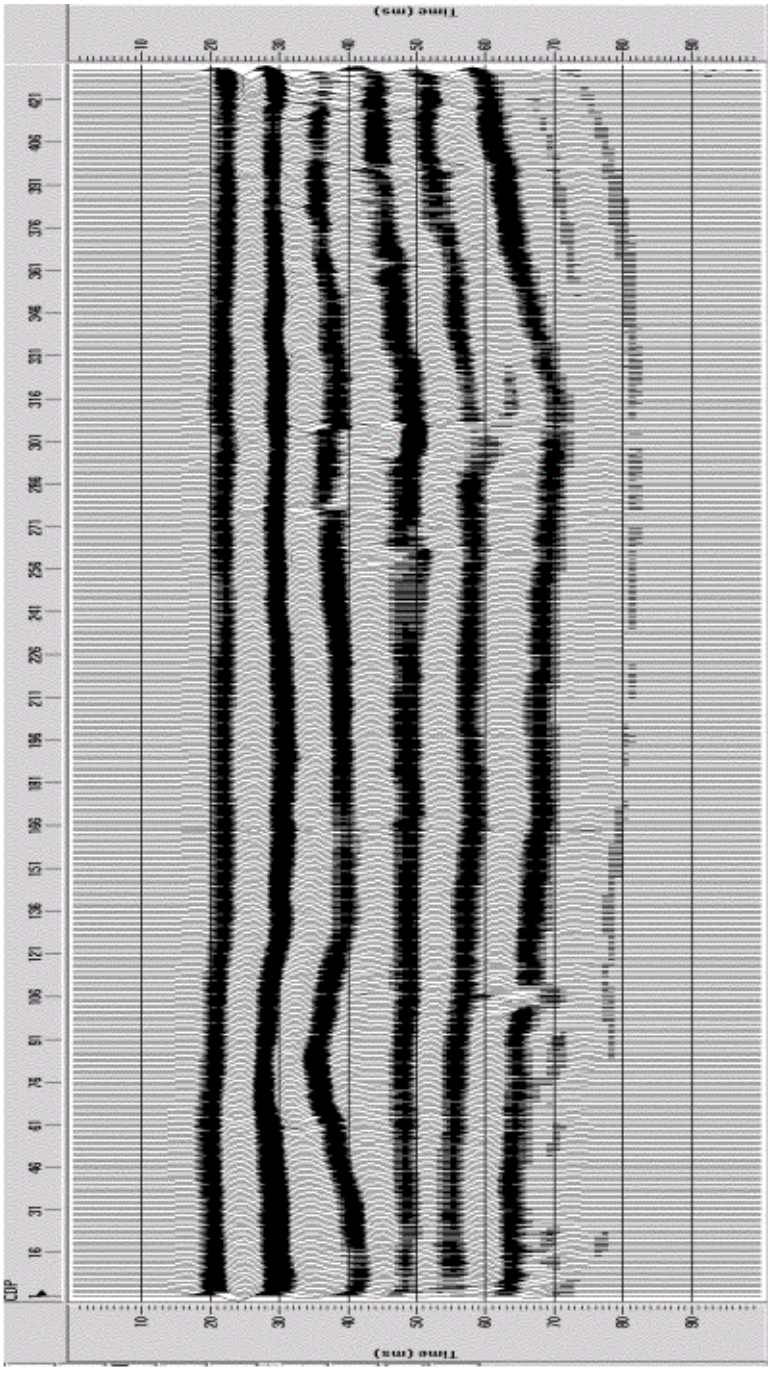

FIG. 16. Seismic traces created with 40 m model, common midpoint ray tracing, 100 Hz wavelet, and migration.

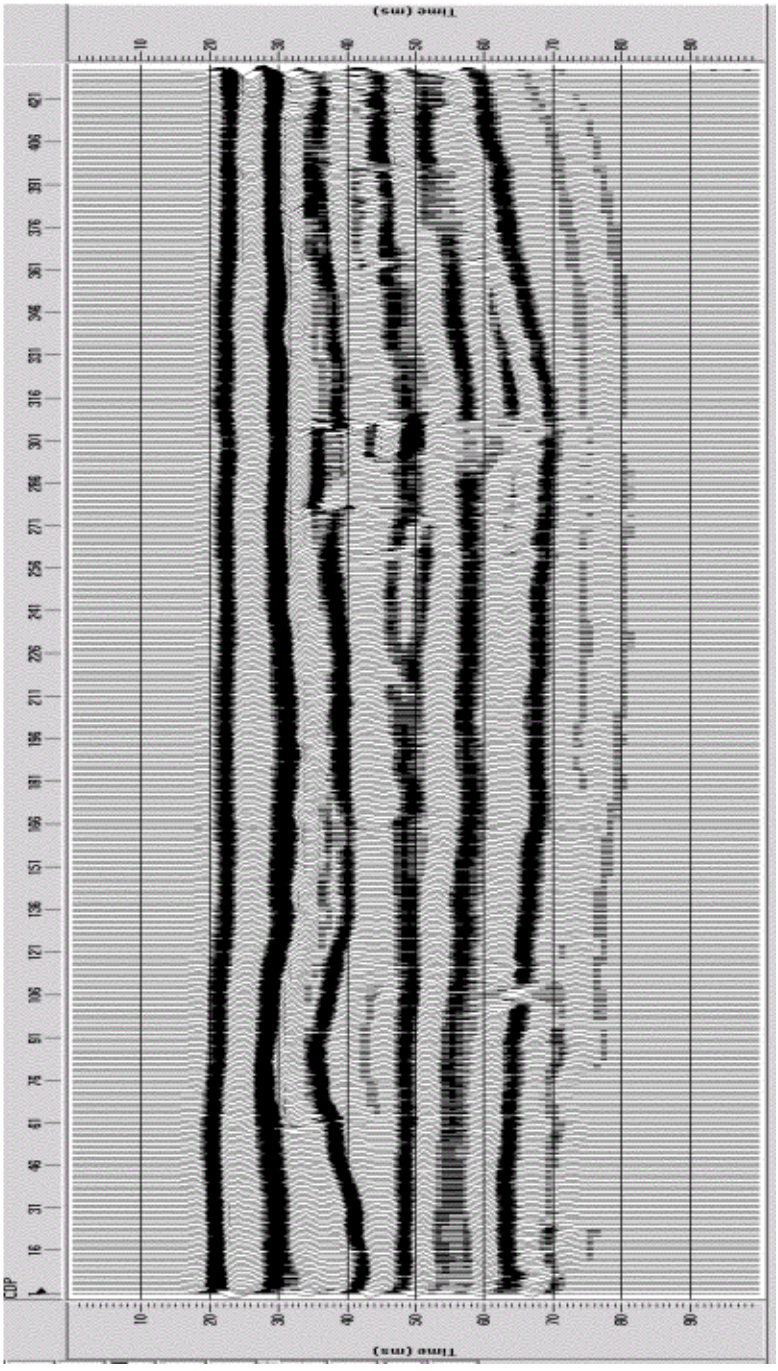

FIG. 17. Seismic traces created with 40 m model, common midpoint ray tracing, 150 Hz wavelet, and migration.

CONCLUSIONS AND RECOMMENDATIONS

The following conclusions and recommendations are drawn from this modelling study:

The coal interval is mappable using seismic reflection techniques, although it is unlikely that individual seams will be resolved in field data, regardless of depth.

Although the coals have large impedance contrasts with respect to the host strata, seismic reflectivity is diminished because individual coal seams are so thin.

Major lateral changes in stratigraphy (such as shale plugs) should be interpretable in field seismic data. However, it is unlikely that IHS units will be resolvable, particularly if the target is at a depth of greater than 100 m.

Optimum depth for the most effective seismic imaging is 200 m. Deeper targets will result in lower dominant frequency in reflection data, and source-generated noise will compromise imaging at depths less than 100 m.

A field test is recommended if the primary objective is the gross structure of the coal interval containing the coal seams, and major lateral facies changes within the coal zone. If the objective is to resolve individual seams as well as IHS strata, then a field test is not recommended.

ACKNOWLEDGEMENTS

The authors would like to thank the Alberta Energy Utilities Board for providing the funding for this study, and Fran Hein at the Alberta Geological Survey for geological input into the modelled cross-section.

REFERENCES

Ainsworth, R.B., 1994, Marginal marine sedimentology and high resolution sequence analysis: Bearpaw – Horseshoe Canyon transition, Drumheller, Alberta: *Bulletin of Canadian Petroleum Geology*, **42**, 1, 26-54.

Gang, T., and Goulty, N.R., 1997, Seismic inversion for coal-seam thicknesses: trials from the Belvoir coalfield, England: *Geophysical Prospecting*, **45**, 535-549.

Gochioco, L.M., 1991, Tuning effect and interference reflections from thin beds and coal seams: *Geophysics*, **56**, 1288-1295.

Gochioco, L.M., 1991, Advances in seismic reflection profiling for U.S. coal exploration: Geophysics, *The Leading Edge*, Dec 1991, 24-29.

Gochioco, L.M, 1992, Modelling studies of interference reflections in thin-layered media bounded by coal seams: *Geophysics*, **57**, 1209-1216.

Gochioco, L.M., 1998, Short Note: Shallow VSP work in the U.S. Appalachian coal basin: *Geophysics*, **63**, 795-799.

Gochioco, L.M., 2000., High-resolution 3-D seismic survey over a coal mine reserve area in the U.S. – A case study: *Geophysics*, **65**, 712-718.

Gochioco, L.M., and Cotton, S.A., 1989, Locating faults in underground coal mines using high-resolution seismic reflection techniques: *Geophysics*, **54**, 1521-1527.

Greaves, R.J., 1984, Coal prospect evaluation using high-resolution reflection seismology – a case study: Geophysics, *The Leading Edge*, Oct 1984, 44-47.

Greenhalgh, S.A., Suprajitno, M., and King, D.W., 1986, Shallow seismic reflection investigation of coal in the Sydney Basin: *Geophysics*, **51**, 1426-1437.

Henson, Jr, H., and Sexton, J.L., 1991, Premine study of shallow coal seams using high-resolution seismic reflection methods: *Geophysics*, **56**, 1494-1503.

Hughes, V.J., and Kennett, B.L.N., 1983, The nature of seismic reflections from coal seams: *First Break*, **9**, 9-18.

Irish, E.J.W.,1970, The Edmonton Group of South-Central Alberta: *Bulletin of Canadian Petroleum Geology*, **65**, 2506-2520.

Knapp, R.W., 1990, Vertical resolution of thick beds, thin beds, and thin-bed cyclothems: *Geophysics*, **55**, 1183-1190.

Knapp, R.W., and Steeples, D.W., 1986, High-resolution common-depth-point reflection profiling: Field acquisition parameter design: *Geophysics*, **51**, 283-294.

Lawton, D.C., 1985, Seismic facies analysis of delta-plain coals from Camrose, Alberta, and lacustrine coals from Pictou Coalfield, Nova Scotia: *American Association of Petroleum Geologists Bulletin*, **69**, 2120-2129.

Lawton, D.C., and Lyatsky, H.V., 1991, Density-based reflectivity in seismic exploration for coal in Alberta, Canada: *Geophysics*, **56**, 139-141.

Lyatsky, H.V., and Lawton, D.C., 1988, Application of the surface reflection seismic method to shallow coal exploration in the plains of Alberta: *Canadian Journal of Exploration Geophysics*, **24**, 124-140.

Rahmani, R.A., 1983, Facies Relationships and Paleoenvironments of a Late Cretaceous Tide-dominated Delta, Drumheller, Alberta: *Field Trip Guidebook 2, Canadian Society of Petroleum Geologists*, Conference on the Mesozoic of Middle America, 36 p.

Rahmani, R.A., 1989, Cretaceous Tidal Estuarine and Deltaic deposits, Drumheller, Alberta: Canadian Society of Petroleum Geologists Field Guide, *Second International Research Symposium on Clastic Tidal Deposits*, August 22-25, Calgary, Alberta, 55 p.

Ramos, A.C.B., and Davis, T.L., 1997, 3-D AVO analysis and modelling applied to fracture detection in coalbed methane reservoirs: *Geophysics*, **62**, 1683-1695.

Rider, M., 1996, *The Geological Interpretation of Well Logs*: Gulf Publishing Company, Houston, 280 pp.

Shepeard, W.W. and Hills, L.V., 1970, Depositional Environments Bearpaw – Horseshoe Canyon (Upper Cretaceous) transition zone, Drumheller "Badlands", Alberta. *Bulletin of Canadian Petroleum Geology*, **18**, 166-215.

Shuck, E.L., David, T.L., and Benson, R.D., 1996, Multicomponent 3-D characterization of a coalbed methane reservoir: *Geophysics*, **61**, 315-330.

Thomsen, R., Tsvankin, I., and Mueller, M.C., 1995, Adaptation of split shear-wave techniques to coalbed methane exploration: *Society of Exploration Geophysicists Annual Meeting*, Exp.Tech.Prog.Abstr.w/biog, **65**, 301-304.

Widess, M.B., 1973, How thin is a thin bed? *Geophysics*, **38**, 1176-1180.